

RESEARCH ARTICLE

# Assessing damages of agricultural land due to flooding in a lagoon region based on remote sensing and GIS: case study of the Quang Dien district, Thua Thien Hue province, central Vietnam

*Đánh giá thiệt hại do ngập lụt đến sử dụng đất nông nghiệp tại vùng đầm phá dựa vào công nghệ viễn thám và GIS: trường hợp nghiên cứu tại huyện Quảng Điền, tỉnh Thừa Thiên Huế, miền Trung Việt Nam*

NGUYEN, Ngoc Bich<sup>1\*</sup>; NGUYEN, Ngu Huu<sup>1</sup>; TRAN, Duc Thanh<sup>1</sup>; TRAN, Phuong Thi<sup>1</sup>; PHAM, Tung Gia<sup>2</sup>; NGUYEN, Tri Minh<sup>3</sup>

<sup>1</sup>University of Agriculture and Forestry, Hue University, 102 Phung Hung Street; Hue City, Vietnam; <sup>2</sup>International School, Hue University, 04 Le Loi, Hue City, Vietnam; <sup>3</sup>Institute of Biotechnology, Hue University, Vietnam

This study aims to create a flood extent map with Sentinel imagery and to evaluate impacts on agricultural land in the lagoon region of central Vietnam. In this study, remote sensing images, obtained from 2017 to 2019, were used to simultaneously map the land cover status of a flood in the Quang Dien district. This study highlights flooded areas from Sentinel-2 images by calculating some indicators such as the Land Surface Water Index (LSWI) and the Enhanced Vegetation Index (EVI). Comparisons between the floodplain samples (GPS point-based) and flood mapping results, with the ground-truth data, indicate that the overall accuracy and Kappa coefficients were 97.9% and 0.62 respectively for 2017; the values for 2019 were 95.7% and 0.77 for the same coefficients. Land use maps overlying the flood-affected maps show that approximately 11% of the agriculture land area was affected by floods in 2019 comparison to a 10% in 2017. Wet rice was the most affected crop with the flooded area accounting for more than 70% of the district under each flood event. The most affected communes are: Quang An, Quang Phuoc and Quang Thanh. This study provides valuable information for flood disaster planning, mitigation and recovery activities in Vietnam.

*Mục tiêu của nghiên cứu là lập bản đồ phân bố ngập lụt với hình ảnh vệ tinh Sentinel và đánh giá ảnh hưởng ngập lụt đến sử dụng đất nông nghiệp ở vùng đầm phá miền Trung, Việt Nam. Trong nghiên cứu này, ảnh viễn thám thu nhận giai đoạn 2017-2019 được sử dụng để xây dựng bản đồ hiện trạng sử dụng đất tại thời điểm bị ngập nước trên địa bàn huyện Quảng Điền. Nghiên cứu đã xác định được vùng ngập lụt ở huyện Quảng Điền bằng phương pháp phân loại chỉ số mặt nước (Land Surface Water Index – LSWI) và chỉ số khác biệt thực vật (Enhanced Vegetation Index-EVI) từ ảnh Sentinel-2. Xác định vùng nước lũ bị che khuất bởi mây bằng mô hình số hóa độ cao (DEM). Kết quả phân loại vùng ngập lụt được so sánh với giá trị tham chiếu mặt đất cho thấy độ chính xác tổng thể và hệ số Kappa đạt được trong năm 2017 là 97,9% và 0,62; trong khi năm 2019 đạt 95,7% và 0,77. Bản đồ sử dụng đất chồng lên bản đồ lũ lụt cho thấy khoảng 11% diện tích đất nông nghiệp bị ảnh hưởng bởi lũ lụt năm 2019 so với 10% năm 2017. Cây lúa nước là cây trồng bị ảnh hưởng nặng nề nhất, với diện tích bị ngập lụt chiếm hơn 70% diện tích lúa của huyện. Các xã bị ngập lớn là xã Quảng An, Quảng Phước và Quảng Thành. Nghiên cứu này cung cấp thông tin có giá trị cho các hoạt động lập kế hoạch, giảm nhẹ và phục hồi thiên tai lũ lụt ở Việt Nam.*

**Keywords:** Remote Sensing & GIS; Sentinel - 2; Flood monitoring; Agricultural land; Central Vietnam.

## 1. Introduction

Floods, droughts and other natural disasters are events frequently occurring in Asia, being categorized as the world's most disaster-prone region (IFRC, 2010). Vietnam is highly susceptible to natural disasters, especially floods, having taken a considerable toll on the country and the people.

According to a World Bank report, natural disasters in Vietnam have taken more than 13,000 lives and approximately 59% of Vietnam's total land area with 71% of its population being susceptible to the impacts of flooding (World Bank, 2010). The lagoon region of central Vietnam is one of the heavily affected areas by flooding; the phenomenon of continuous high tides has made flooding more serious.

\* Corresponding author  
Email: nguyenbichngoc@huaf.edu.vn

In the Central region, an average of 12,000 hectares of rice cultivation are flooded each year (about 5,000 hectares are lost and 7,000 hectares are affected); more than 6,200 hectares of other crops are also inundated (Nguyen Lap Dan & Nguyen Thi Thao Huong, 2007). Flood frequencies and intensities have increased over the past few decades due to climate change (Ermolieva & Sergienko, 2008; IPCC, 2007). Therefore, there is an increase in the researchers' interest in flood monitoring and flood damage assessment (Pantaleoni et al., 2007).

Traditional methods, relying on ground surveys and aerial observations, have been applied for flood mapping. However, if the flood is extensive, an accurate monitoring of the flood event is challenging due to the bad weather conditions. Moreover, these traditional methods tend to be time-consuming, expensive and necessitates some degree of experience for their application. Nowadays, satellite data is an effective solution to replace the traditional methods in monitoring these events and the flooding level in particular areas (Brivio et al., 2002). In addition, Geographic information systems (GIS) combined with remote sensing (RS) techniques have demonstrated to be a very effective approach in the analysis of flood areas and the risks over inundated areas (Sarker MZ, 2011; Uddin et al., 2013). Remote sensing is an important source of data (Dano Umar et al., 2011); it is an easy way to collect and analyze relevant data and to save time and workforce as well (Nicandrou, 2010). This paper aims to create a flood inundation extent mapping for the years of 2017 and 2019 with Sentinel imagery in the lagoon region of Central Vietnam. The goal is to estimate the most affected land cover types and to assess damages to agriculture land.

## 2. Materials and methodologies

### 2.1. Site selection

The study area is located between 107°E 24' to 107°34' E and 16°N31' to 16°N, approximately 15 km northeast of Hue City, in the lowland and coastal region of Central Vietnam (Figure 1). The Quang Dien district lies in the floodplain delta of two major river basins: the Huong and the Bo. The climate is tropical with two distinctive seasons: dry and wet. From September to December, the wet season has an average rainfall of 2,500 mm with a humidity average of 85%. The agricultural sector is vital in province since nearly all agriculture production is consumed locally (Thua Thien Hue Statistics Office, 2019).

The 2017 and 2019 floods were severe in both, their magnitude and duration, with significant impacts not only on the natural aspects but also on the economic and social issues. In 2017, a sudden flood in the Quang Dien district submerged 30 hectares of crops at the most massive vegetable bowl in the Quang Thanh commune and more than 25 hectares of rice in Sia town, the Quang Phuoc and the Quang An communes.

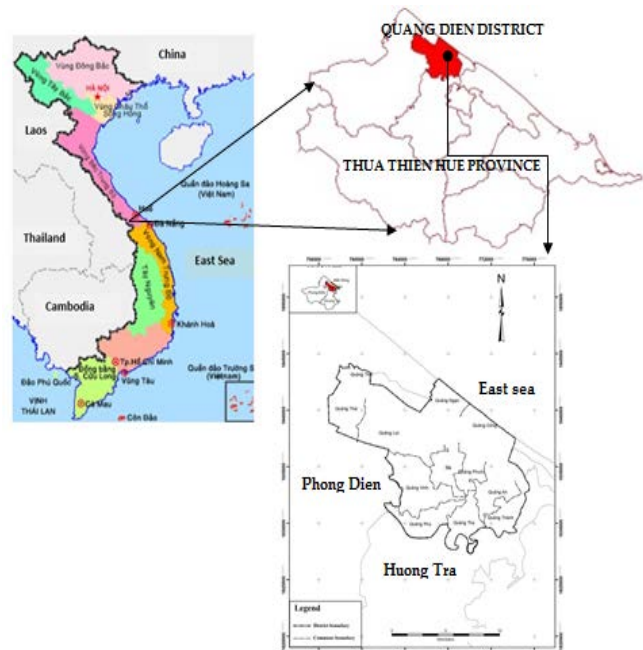


Figure 1. Location map of the study area

In November 2019, the administration of the Quang Dien district evacuated 129 households with more than 255 people. Floods caused the loss of 100 hectares of winter crops and over 5,000 banana trees. Severe landslides occurred in dikes and inland canals in Quang Phu, Quang Tho, Quang An, Quang Phuoc and Quang Thanh communes (Quang Dien People's Committee, 2017, 2019).

### 2.2. Data

#### 2.2.1. Satellite data

Sentinel-2A is a part of the European Copernicus program created by the European Space Agency (ESA). Sentinel-2A has a good spatial and spectral resolution in the near-infrared region and three Vegetation Red Edge bands with 20-meter spatial resolution. However, it does not offer thermal data nor a panchromatic band. The satellites' major objective is to observe and monitor land and ocean surfaces at day and night under all weather conditions (D'Odorico et al., 2013).

Sentinel-2A images of 2017 and 2019 were freely gathered from the Copernicus program (formerly known as Global Monitoring for Environment and Security (GMES) from its website (<https://scihub.copernicus.eu/dhus>)). According to the reports of the Quang Dien People's Committee, in 2017 and 2019, floods took place in September and November respectively, causing serious damages to agricultural production. The images were collected in September and November, improving the identification of wetlands. The dates of the images are: 16 September 2017, 06 November 2017, 03 September 2019 and 12 November 2019 with a resolution of 20 m x 20 m.

The Sentinel data was used to estimate the Enhanced Vegetation Index (EVI) and the Land Surface Water Index (LSWI) of the study areas. By estimating the extent of paddy fields, Xiao et al. (2005, 2006) identified pixels representing flooding from the difference between the LSWI and EVI.

### 2.2.2. Ancillary and ground reference data

From 2017 to 2019, two field surveys were conducted in the flooded land of the Quang Dien district. All the observation sites (200 in total), distributed within the Quang Dien plain, were utilized to assess the flood mapping accuracy. Digital photographs and GPS data were obtained by field investigation and were used to verify the accuracy of the land cover classification. Statistics of the agricultural land (of 2017 and 2019) were also collected from the Office of Natural Resources and Environment Department of the Quang Dien district; statistics data was used for accuracy verification of the classification results.

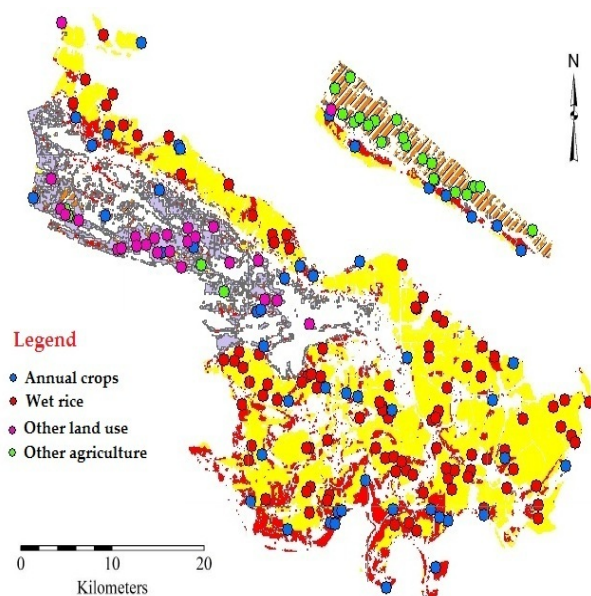


Figure 2. Map showing GPS sample points

## 2.3. Research methods

### 2.3.1. Identification of the water surface using EVI and LSWI

Xiao et al. (2005, 2006) applied an algorithm on anomalies between the Land Surface Water Index (LSWI) and Vegetation Indexes (NDVI and EVI) to estimate the distribution of paddy fields in South China and South and Southeast Asia (Xiao et al., 2005, 2006). In accordance with their approaches, in this study a methodology is proposed to detect the spatial-temporal flood distribution in the lagoon region of central Vietnam; the methodology is based on the smoothing of indexes derived from these differences. The equations used to derive the EVI (Huete et al., 1997) and the LSWI (Ceccato et al., 2002) are as follows:

$$EVI = 2.5 * \frac{NIR - RED}{NIR + 6 * RED - 7.5 * BLUE + 1} \quad (1)$$

$$LSWI = \frac{NIR - SWIR}{NIR + SWIR} \quad (2)$$

where NIR is the surface reflectance value: 0–1.0 in the near infrared (841–875 nm, Band 2), RED (621–670 nm, Band 1), BLUE and (459–479 nm, Band 3). SWIR is the short-wave infrared (1628–1652 nm, Band 6); gain factor = 2.5. In the present study, the approach is applied to the EVI and LSWI time-series as well as the differences between them to reduce the noise component and to interpolate missing information. This was undertaken to determine spatial-temporal changes in flooding areas within the lagoon region during the period from 2017 to 2019.

### 2.3.2. Classify image series EVI, LSWI to create flood maps

In accordance with the pioneering method described by Xiao et al. (2005, 2006), the difference between EVI and LSWI (DVEL) was used in the present study to discriminate Water-related pixels from Non-flood pixels.

$$DVEL = EVI - LSWI \quad (3)$$

If the smoothed DVEL is less than 0.05, such pixels are determined to be a Water-related pixel; however, the smoothed DVEL data for the lake and sea are not always less than 0.05. The high DVEL may reflect low LSWI caused by extremely low reflectance (near 0) of open water in the NIR band. To solve this problem, the following criteria was empirically added to avoid such misclassifications: (1) if the smoothed EVI is less than or equal to 0.05 and the smoothed LSWI is less than or equal to 0, the pixel is determined as a Water-related pixel; (2) if the EVI is greater than 0.3, the pixel is categorized as a Non-flood pixel. Water-related pixels were divided into two categories (Flooded and Long-term water bodies) based on the following simple method.

The EVI, in homogeneous open-water areas such as large lakes or the sea, is generally lower than its value for mixed pixels (a mix of water, vegetation and soil coverage). This study assumed that a water-related pixel is a mixture of flood water and other land use targets. Thus, if the smoothed EVI was less than or equal to 0.1, the water-related pixels were defined as Flood pixels.

Land-based aquaculture is widely distributed throughout coastal areas. This study only focuses on temporal changes in annual flooding, therefore, these areas and those with an extended inundation period (rivers, lakes, and the sea) were discriminated from the areas subjected to short-term and seasonal inundation. Considering that the yearly aquaculture period lasts from 3 to 4 months in coastal areas, these areas were empirically defined as follows: If

the total number of days as a water-related pixel is greater than or equal to 250 days per year, the pixels are classified as long-term water bodies.

### 2.3.3. Agricultural land classification

Land cover is an important factor to identify those zones that have shown high susceptibility to flooding (Norman et al., 2010). Vegetated areas have a low potential for flooding due to the negative relationship between flooding and vegetation density. On the other hand, residential areas and roads, which mostly are impervious surfaces and bare lands, increase the storm runoff (Tehrany et al., 2013). Based on information recorded from field surveys, results documented in the literature and ancillary data, six land covers were selected for classification: rice, annuals crops, aquaculture, forest and perennial crops, other land uses, rivers and lakes. In this study, we used the GIS&RS technology to map land use and to measure the extent of flooding affecting agricultural land. The inundated land was then identified by the overlay of the flood extension layer over the agricultural land use layer.

### 2.3.4. Accuracy assessment

In order to determine the reliability of the classification results, the accuracy was calculated comparing the classified image data and the field data set according to the error matrix construction method. The accuracy assessment was carried out using 200 points, based on ground truth data and visual interpretation. The comparison of reference data and classification results was statistically carried out by error matrices. The reliability of the results was estimated through the calculation of two indexes: the global accuracy and the Kappa index. The Kappa index is a measure of agreement between predefined produced ratings and the user assigned ratings. It is calculated by a formula:

$$K = \frac{P(A) - P(E)}{1 - P(E)} \quad (4)$$

where P(A) is the global precision given by the error matrix.  $P(A) = \text{Sum of the diagonal quantities} / \text{Sum of the row (column) quantities}$ ; P(E) is a quantity representing the desire (expected) for a predictable precision classification; P(E) contributes to the estimation of the accuracy of the classification in the actual classification (Gwet, 2002).

## 3. Results and discussions

### 3.1. Flood-affected area classification results

The spatial extent of the inundation changes during the flooding can be visualized and assessed by the display of successive maps. This has been done for the 2019 and 2017 floods in the lagoon region of central Vietnam (Figure 3). The estimated flood area is shown for September and

November during the floods of 2017 and 2019. In 2017, there were two floods started following a rapid increase in the water level in 16 September and 06 November. The floods of 2019 started similarly as the floods in 2017. However, in 2019, the water level and the resulting inundation area increased on 03 September and 12 November.

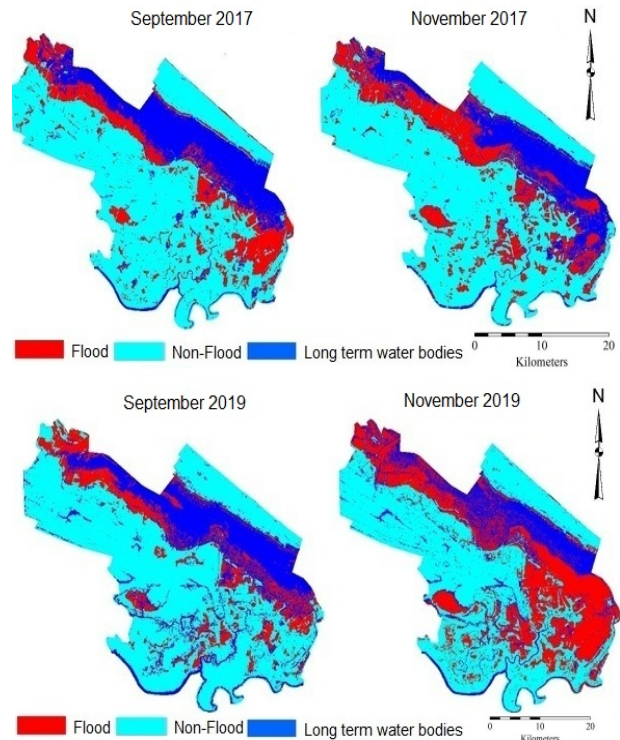


**Figure 3. Spatial distribution of the flood-inundated area during the months of September to November of 2017 and 2019**

The images also show how much the spatial-temporal distribution of the inundated area varies in time. The classification results show the spatial distribution of the areas affected by floods in 2017, compared to those from 2019 (Figure 4).

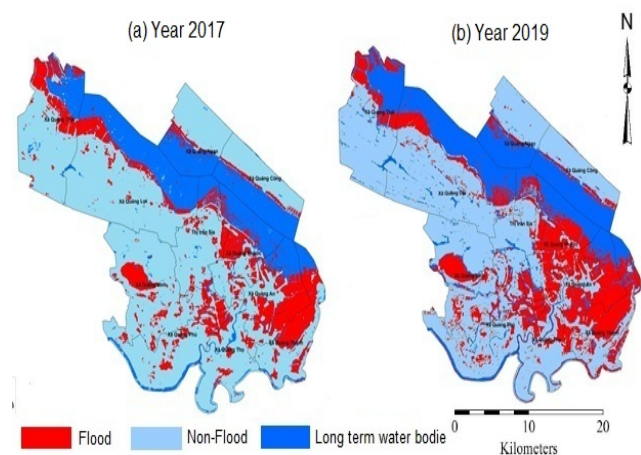


**Figure 4. Flood inundation map of Quang Dien district using Sentinel-2 images for (a) the Year 2017 and (b) the Year 2019.**

In general, flood-affected areas were distributed along the main rivers, especially in the southern part of the region. The area affected by floods in 2017, was estimated at approximately 903.3 ha, while that for 2019 was larger (943.98 ha).

The comparison between the flood mapping results and the ground reference data for 2017 indicated an overall accuracy of 97.9% and a Kappa coefficient of 0.62. The values for 2019 were 95.7% and 0.77 respectively. We also verified the mapping results by comparing the Sentinel derived flood-affected areas with those of the water level gauging station as reference data at the provincial level. These results confirm a robust fitting between the two datasets. Figure 5 shows the water level measured during the inundation periods of 2017 and 2019, ranging from more than 150 cm to nearly 400 cm. The flooded areas range from over 200 ha to nearly 700 ha. The comparison shows the compatibility between the two data sets, the flooded area determined from Sentinel images and the fluctuation of the water level measured at the gauging station.

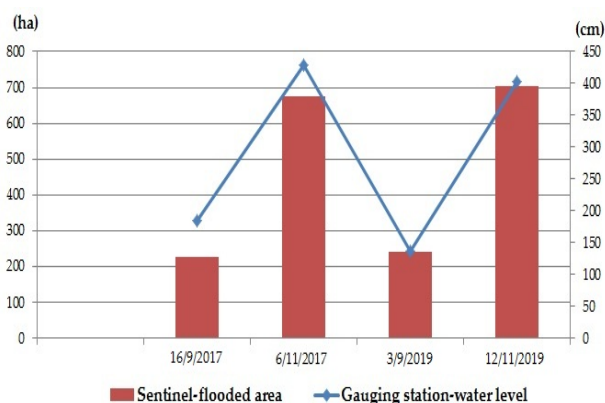


Figure 5. Analysis obtained from comparisons between the Sentinel-derived flooded area and the gauging station-water level.

There is a close correlation between the flooded area and the measured water level at Phu Oc observation station. This indicates that, the higher the water level, the greater the flooded area in the Quang Dien district. This result also reflects the local reality. In general, the maximum extent of areas prone to flood inundation is shown during the floods in 2017 and 2019. The red, light blue and blue colors represent areas of flood, non-flood and long-term water bodies respectively. It is evident that the extent of the flooding varies from year to year.

The common areas from both significant floods are classified as the most vulnerable areas. The information regarding flooding potential vulnerability could be useful for many purposes such as: flood monitoring, preparation of crop calendars and damage assessment on agricultural land. We highlight that these results solely focused on the damage impact of flood on agricultural land use in the lowland region of the Quang Dien district.

### 3.2. Land use cover classifications

Crop classification showed the spatial distribution of agriculture cropping systems during 2017 and 2019, generally comparable for both years. Outcomes from the pixel-by-pixel comparison between the classification results and the ground reference data, indicate that the overall accuracy and Kappa coefficient achieved for the 2017 data were 84.1% and 0.76 respectively. Those obtained for 2019 were 88.5% and 0.82.

The lower accuracy level was observed for perennial crops since this class occupies small areas and is spatially scattered across the region. Moreover, its pattern was often confused with those of field crops due to mixed pixel issues, potentially being omitted from the interpretation results. Additionally, we compared the classification results with the government land use area statistics at a district level to examine the correlation between the two datasets, revealing a close agreement (Figure 6).

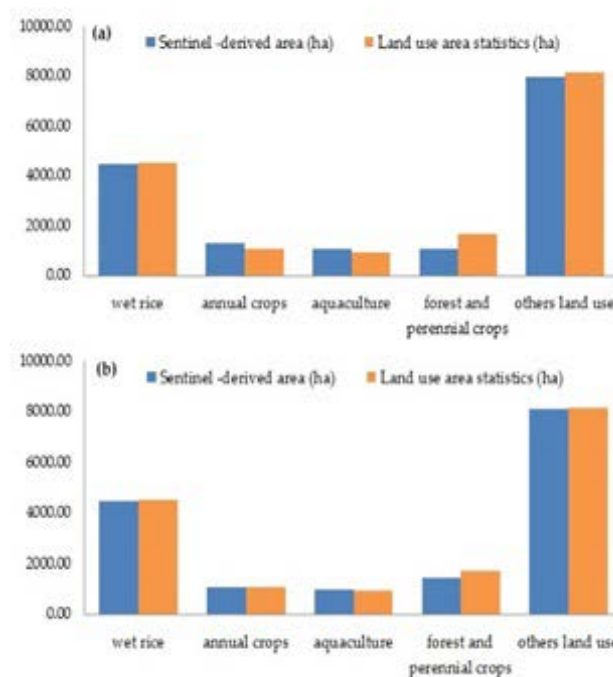


Figure 6. Analysis results obtained from comparisons between the Sentinel-derived area and the land use area statistics: (a) 2017 and (b) 2019.

### 3.3. Damage assessment of agricultural land

This study assessed the impact of 2017 and 2019 floods on agricultural land use in the Quang Dien district. While results of agricultural effects are presented for each flood, the inundation maps for the years 2017 and 2019 are presented in this paper. The land use maps were overlaid on the flood-affected area maps to delineate the crop cultivation areas affected by floods. From these maps, it can be seen that inundation occurs in the low areas of the two main river systems (Huong and Bo River) affecting ten communes and one town. Among them, the most affected communes are Quang An, Quang Phuoc, and Quang

Thanh. Regarding types of land cover, the paddy land type is the most affected followed by annual crop lands identified in Figure 7.

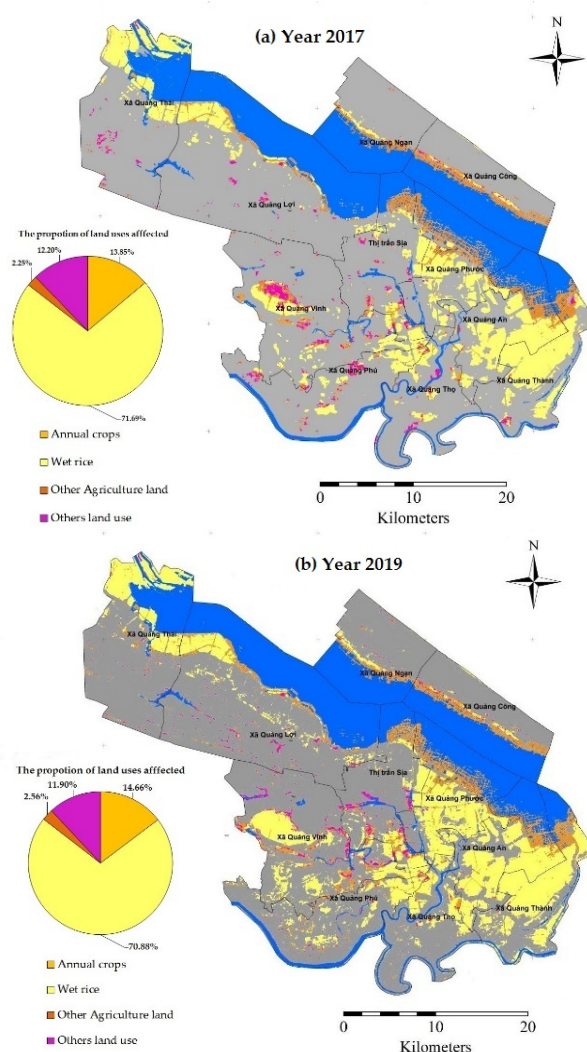


Figure 7. Different land uses in Quang Dien districts affected by 2017 (a) and 2019 (b) flood events.

According to the results, agricultural land was the land use most impacted by floods among all of the inundated land use classes. Each flood led to more than 90% of the inundated areas being agricultural land; the remaining 10% belong to other land use types, including industrial and commercial land. The 2017 flood event submerged 793.08 ha, representing 10% of the total agricultural area in Quang Dien. The entire affected area increases to 11% (831.62 ha) of total agricultural land in the year 2019, probably due to the flood-induced damage of rainy season crops. Overall, each of the floods led to just more than 80% of the inundated area being rice land. The second largest affected land use type is the annual crops land (16% for the 2017 flood and 17% for 2019 flood); approximately 3% of the inundated area is under other agriculture land uses.

The result of agricultural land in the Quang Dien district that would be inundated under the two flooding events is presented in Table 1. Wet rice is the crop most affected. The flooded agricultural land increases significantly as the flooding intensity rises; from 14% during the 2017 flood to 15% in 2019. Despite rice crops are more vulnerable to long periods of inundation, they also can better recover than the annual crops such as maize, sweet potatoes, sesame, beans and other vegetables that are more sensitive to the effects of the inundation.

This study is based on methodology developed by Xiao and colleagues to detect the spatial extents and temporal changes of flood inundation in central Vietnam during the rainy season. Using this modified methodology, Sentinel satellite images were used to develop flood inundation maps for the floods of 2017 and 2019.

Remotely sensed data can be used effectively in flood detection and mapping. The flood region detection was satisfactory, indicating that the approach of EVI and LSWI during an optimum temporal window holds great potential in flood mapping. The analyses in this paper can improve our understanding about the impact of floods in lowland regions such as the lagoon or any other regions presenting similar conditions as of Thua Thien Hue province.

Table 1. Calculated areas of agricultural land in Quang Dien district affected by flood

Land use type	Total area (ha)		Flooded area (ha)		Flooded area (%)		% of total district agricultural land	
	2017	2019	2017	2019	2017	2019	2017	2019
Annual crops*	1308.94	1084.31	125.14	138.37	16	17	10	13
Wet rice	4471.80	4443.40	647.60	669.10	82	80	14	15
Other agriculture	2130.56	2383.59	20.34	24.15	3	3	1	1
Sub total	7911.30		793.08	831.62			10	11

\*Annual crops are predominately by corn, beans, peanut, cassava, sweet potatoes and other vegetables

#### 4. Conclusions

The findings from this study have validated the mapping approaches for delineating flood-affected agriculture land from the sentinel data. Comparisons between the flood land samples (GPS points) and based flood mapping

results, with the ground reference data, indicated that the overall accuracy and Kappa coefficient achieved for the 2017 flooding were 97.9% and 0.62 respectively. Those from the 2019 event were 95.7% and 0.77. The application of EVI data for land use classification in 2017 and 2019 indicated satisfactory results.

The flood-affected area maps, compared with the land use maps, indicate the area of agriculture land affected by floods occurring in 2017 and 2019. Results indicate that 10% and 11% of the agriculture land use area were affected by such floods. The largest proportion of flood-affected area (15%) was observed for wet rice in 2019. The flood areas were spatially scattered across the region along main rivers. These methods could provide quantitative information on agriculture land affected by floods, which is important for monitoring purposes. These conclusions are useful in land use planning and agriculture adaptations due to floods for local governments.

## 5. References

- [1] Brivio, P. A., Colombo, R., Maggi, M., & Tomasoni, R. (2002). Integration of remote sensing data and GIS for accurate mapping of flooded areas. *International Journal of Remote Sensing*, 23(3), 429–441.
- [2] Ceccato, P., Flasse, S., & Grégoire, J.-M. (2002). Designing a spectral index to estimate vegetation water content from remote sensing data: Part 2. Validation and applications. *Remote Sensing of Environment*, 82(2), 198–207.
- [3] D’Odorico, P., Gonsamo, A., Damm, A., & Schaepman, M. E. (2013). Experimental evaluation of Sentinel-2 spectral response functions for NDVI time-series continuity. *IEEE Transactions on Geoscience and Remote Sensing*, 51(3), 1336–1348.
- [4] Brivio, P. A., Colombo, R., Maggi, M., & Tomasoni, R. (2002). Integration of remote sensing data and GIS for accurate mapping of flooded areas. *International Journal of Remote Sensing*, 23(3), 429–441.
- [5] Ceccato, P., Flasse, S., & Grégoire, J.-M. (2002). Designing a spectral index to estimate vegetation water content from remote sensing data: Part 2. Validation and applications. *Remote Sensing of Environment*, 82(2), 198–207.
- [6] D’Odorico, P., Gonsamo, A., Damm, A., & Schaepman, M. E. (2013). Experimental evaluation of Sentinel-2 spectral response functions for NDVI time-series continuity. *IEEE Transactions on Geoscience and Remote Sensing*, 51(3), 1336–1348.
- [7] Dano Umar, L., Matori, A. N., Hashim, A. M., Chandio, I. A., Sabri, S., Balogun, A. L., & Abba, H. A. (2011). Geographic information system and remote sensing applications in flood hazards management: a review. *Research Journal of Applied Sciences, Engineering and Technology*, 3(9), 933–947.
- [8] Ermolieva, T. Y., & Sergienko, I. V. (2008). Catastrophe risk management for sustainable development of regions under risks of natural disasters. *Cybernetics and Systems Analysis*, 44(3), 405.
- [9] Gwet, K. (2002). Kappa statistic is not satisfactory for assessing the extent of agreement between raters. *Statistical Methods for Inter-Rater Reliability Assessment*, 76(1), 378–382.
- [10] Huete, A. R., Liu, H. Q., Batchily, K., & van Leeuwen, W. (1997). A comparison of vegetation indices over a global set of TM images for EOS-MODIS. *Remote Sensing of Environment*, 59(3), 440–451.
- [11] IFRC. (2010). (International Federation of Red Cross and Red Crescent Societies). *Disasters in Asia: The case for legal preparedness* Geneva.
- [12] IPCC. (2007). *Climate change 2007: The physical science basic. Contribution of working group I to the fourth assessment report of Intergovernmental Panel on climate change*. Cambridge, UK: Cambridge University Press.
- [13] Nguyen Lap Dan, Nguyen Thi Thao Huong, V. T. T. L. (2007). *floods in Central Vietnam causes and preventive solutions*. Science-Nature and Technology Ha Noi, 264.
- [14] Nicandrou, A. (2010). *Hydrological assessment and modelling of the River Fani Catchment*, Albania. University of Glamorgan.
- [15] Norman, L. M., Huth, H., Levick, L., Shea Burns, I., Phillip Guertin, D., Lara-Valencia, F., & Semmens, D. (2010). Flood hazard awareness and hydrologic modelling at Ambos Nogales, United States–Mexico border. *Journal of Flood Risk Management*, 3(2), 151–165.
- [16] Pantaleoni, E., Engel, B. A., & Johannsen, C. J. (2007). Identifying agricultural flood damage using Landsat imagery. *Precision Agriculture*, 8(1–2), 27–36.
- [17] Quang Dien People’s Committee. (2017). *Flood prevention, response and rehabilitation report 2017*. Quang Dien district.
- [18] Quang Dien People’s Committee. (2019). *Flood prevention, response and rehabilitation report 2019*. Quang Dien district.
- [19] Sarker MZ, S. A. (2011). GIS and RS combined analysis for flood prediction mapping – a case study of Dhaka City Corporation, Bangladesh. *Electr Control Eng*, 1, 250–257.
- [20] Sentinel, E. (n.d.). *Delivers First Images*. Available online: [http://www.esa.int/Our\\_Activities/Observing\\_the\\_Earth/Copernicus/Sentinel-2/Sentinel-2\\_delivers\\_first\\_images](http://www.esa.int/Our_Activities/Observing_the_Earth/Copernicus/Sentinel-2/Sentinel-2_delivers_first_images).
- [21] Tehrany, M. S., Pradhan, B., & Jebur, M. N. (2013). Spatial prediction of flood susceptible areas using rule-based decision tree (DT) and a novel ensemble bivariate and multivariate statistical models in GIS. *Journal of Hydrology*, 504, 69–79.
- [22] Thua Thien Hue Statistics Office. (2019). *Thua Thien Hue statistical yearbook 2019*. Thua Thien Hue: Statistical Publishing House.

- [23] Uddin, K., Gurung, D. R., Amarnath, G., & Shrestha, B. (2013). Application of Remote Sensing and GIS for Flood Hazard Management: A Case Study from Sindh Province, Pakistan. *American Journal of Geographic Information System*, 6(2), 1–5.
- [24] World Bank. (2010). *Weather the storm: Option for disaster risk financing in Vietnam*. Washington, D.C.
- [25] Xiao, X., Boles, S., Froking, S., Li, C., Babu, J. Y., Salas, W., & Moore, B. (2006). Mapping paddy rice agriculture in South and Southeast Asia using multi-temporal MODIS images. *Remote Sensing of Environment*, 100(1), 95–113.